

Luminosity and mass limits for the progenitor of the type Ic supernova 2004gt in NGC 4038

Justyn R. Maund

Institute of Astronomy, University of Cambridge, Madingley Road, Cambridge CB3 0HA, England, U.K.

jrm@ast.cam.ac.uk

and

Stephen J. Smartt

Department of Physics and Astronomy, Queen's University Belfast, Belfast, BT7 1NN, Northern Ireland, U.K.

s.smartt@qub.ac.uk

and

Francois Schweizer

Carnegie Observatories, 813 Santa Barbara Street, Pasadena, California 91101 USA

schweizer@ociw.edu

ABSTRACT

We report our attempts to locate the progenitor of the type Ic SN 2004gt in NGC 4038. We use high resolution HST ACS images of SN 2004gt and have compared them with deep pre-explosion HST WFPC2 F336W, F439W, F555W and F814W images. We identify the SN location on the pre-explosion frames with an accuracy of 5mas. We show that the progenitor is below the detection thresholds of all the pre-explosion images. These detection limits are used to place luminosity and mass limits on the progenitor, by comparing them with stellar evolution tracks on the Hertzsprung-Russell diagram. The progenitor of SN 2004gt seems to be restricted to a low-luminosity high-temperature star, either a single WC star with initial mass $> 40M_{\odot}$ or a low mass star in a binary. The pre-explosion data cannot distinguish between the two scenarios.

Subject headings: stars:evolution—supernovae:general—supernovae:individual(2004gt)—galaxies:individual(NGC 4038)

1. INTRODUCTION

Stellar-evolution models predict that all stars with $M_{ZAMS} \gtrsim 8M_{\odot}$ should end their lives in a core-collapse induced supernova (CCSN) explosion (e.g. Heger et al. (2003); Eldridge & Tout (2004)). The identification of the progenitor of a CCSN just prior to explosion provides a critical test for models of stellar evolution. The task of finding the progenitors is complicated by the unpredictable nature of SNe. The two nearby supernovae SN 1987A (Walborn et al. 1989) and SN 1993J (Aldering et al. 1994) had progenitors identified shortly after discovery. Modern telescope archives have allowed the search for progenitors to be increased to large distances (Maund & Smartt 2005; Van Dyk et al. 2003). In order to confidently identify the correct star as a SN progenitor on images of the highest resolution, precise astrometric techniques are required. Recently, Maund & Smartt (2005) and Smartt et al. (2004) have used high resolution post-explosion images with the Hubble Space Telescope (HST) and the technique of differential astrometry to accurately identify progenitors on pre-explosion HST images. The brightness and colour information from pre-explosion images may then be used to place the progenitor on the Hertzsprung-Russell (HR) diagram (e.g SN 2003gd, Smartt et al. 2004; SN 1999ev, Maund & Smartt 2005). There are no detections yet of progenitors of the hydrogen deficient SNe Ib or Ic, although upper limits to their absolute magnitudes have been determined (see §4). It is now thought that some SNe Ic produce gamma-ray bursts (GRBs; Matheson et al. 2003; Hjorth et al. 2003), and that the progenitors may be rapidly rotating massive Wolf-Rayet (WR) stars.

This letter presents the study of HST Wide Field Planetary Camera 2 (WFPC2) images of the site of SN 2004gt in the interacting galaxy NGC 4038, prior to explosion. SN 2004gt was discovered by L.A.G. Monard (Monard et al. 2004) on 2004 Dec 12.076 with an unfiltered magnitude of 14.6, corresponding to an absolute magnitude of ≈ -17 at the distance of NGC 4038 ($(m - M)_0 = 31.4$; Whitmore et al. 1999). The position of SN 2004gt was given as $\alpha_{2000} = 12^h 01^m 50^s.37$, $\delta_{2000} = -18^{\circ} 52' 12.''7$. Ganeshalingam et al. (2004) classified SN 2004gt of Type Ic. The WFPC2 data are the deepest, and widest wavelength coverage, pre-explosion images of any nearby SNe Ibc to date, and provide a unique opportunity to study the progenitor site of a possible Gamma Ray Burst (GRB)-related supernova event.

2. OBSERVATIONS AND DATA ANALYSIS

The pre- and post-explosion HST observations of the site of SN 2004gt are listed in Table 1. The pre-explosion WFPC2 observations (Programme G0-5962; PI: B. Whitmore), in each filter, are drizzled combinations of four separate exposures. These four exposures were acquired in pairs, for the rejection of cosmic rays, with an offset of $0.25''$ between pairs of

exposures (Whitmore et al. 1999). The progenitor of SN 2004gt fell on the Planetary Camera (PC) chip for which the pixel size of the drizzled image was $0.025''$ (the same as the HST Advanced Camera for Surveys (ACS) High Resolution Channel (HRC)). Aperture photometry was performed on the final images using the IRAF implementation of DAOPHOT and the prescription of Whitmore et al. (1999). Empirical aperture corrections were calculated for each frame and small charge transfer inefficiency corrections (~ 0.01 mag) were applied to the photometry using the prescription of Dolphin (2000a). The photometry was converted to the standard Johnson-Cousins system using the transformations of Holtzman et al. (1995) with the updates of Dolphin (2000b).

DAOPHOT provides four centering algorithms to calculate the locations of stars: centroid, ofilter, Gaussian and PSF fitting. The scatter in the measured locations of stars was used to describe the uncertainty due to the under-sampled PSF of WFPC2.

Post-explosion ACS images (Programme GO-10187; PI: S. Smartt) were analysed using the PYRAF implementation of DAOPHOT, using Tiny Tim PSFs (Krist & Hook 2004) for PSF photometry. Empirical aperture corrections to $0.5''$ were calculated for each frame (with the aperture correction for $0.5''$ to ∞ taken from Sirianni et al. (2005)), and the photometry was corrected for charge transfer inefficiency according to the relationships of Riess & Mack (2004). The photometry was converted from the ACS VegaMag system to standard Johnson-Cousins magnitudes using the transformations of Sirianni et al. (2005). The photometry was found to agree with results from the DOLPHOT package (Dolphin 2000b) to $\lesssim 0.1$ mag at $m \approx 25$.

The locations of 16 stars common to both the pre-explosion WFPC2 imaging and the post-explosion ACS imaging were used to calculate the transformation between the two sets of F555W images, using the IRAF task *geomap*. The transformation uncertainty was calculated as:

$$(\Delta r_2)^2 = (\sigma_1)^2 + (\sigma_2)^2 + \Delta T^2, \quad (1)$$

where a position is being transformed from frame 1 to frame 2 and Δr_2 is the uncertainty of the final transformed position, σ_1 and σ_2 are the mean scatters in the positions of the stars used for the geometric transformation, from the four centering techniques employed by DAOPHOT, and ΔT is the r.m.s. scatter on the transformation. The positions of stars on the ACS frame were transformed to the coordinates of the drizzled PC F555W image with an accuracy of ± 5 mas. The reverse transformation has an uncertainty of ± 4.6 mas. SN 2004gt is located $1.3''$, approximately South, from knot S(Whitmore et al. 1999).

3. OBSERVATIONAL RESULTS

SN 2004gt is readily identifiable on post-explosion ACS images. We measure the apparent brightness and colours of SN 2004gt on 2005 May 16 as $m_V = 18.55 \pm 0.12$, $B - V = 0.87 \pm 0.16$ and $V - I = 1.32 \pm 0.15$. The location of SN 2004gt and its position on the WFPC2 pre-explosion images are shown as Fig. 1. The limiting magnitude at the position of SN 2004gt on the pre-explosion frames was determined using the technique of Maund & Smartt (2005). Aperture photometry was done over a 9-point grid centered at the SN position, with offsets of 1 pixel which permitted background variations, over the aperture area, to be taken into account. The detection thresholds determined in this manner were tested by adding a scaled PSF at the SN position on the pre-explosion magnitude. This tested if the DAOPHOT photometry would recover a star at the calculated detection threshold. The detection thresholds were determined to be: $m_{F336W} = 23.04$, $m_{F439W} = 24.56$, $m_{F555W} = 25.86$ and $m_{F814W} = 24.43$.

The post-explosion ACS photometry of stars within $2''$ was used to estimate the reddening towards SN 2004gt using the technique of Maund & Smartt (2005). The photometry of 47 nearby stars was used to estimate the reddening as $E(B - V) = 0.07 \pm 0.01$. This low reddening is consistent with the foreground reddening as quoted by NED¹, after Schlegel et al. (1998).

The detection thresholds, calculated above, were converted to absolute magnitudes taking into account the distance and extinction towards NGC 4038. We calculated the extinctions in WFPC2 bands, using the $A_X/E(B - V)$ relations of Van Dyk et al. (1999), to be: $A_{F336W} = 0.39$, $A_{F439W} = 0.30$, $A_{F555W} = 0.20$ and $A_{F814W} = 0.13$. This implies the progenitor on the pre-explosion frames had magnitudes: $M_{F336W} \gtrsim -8.75$, $M_{F439W} \gtrsim -7.14$, $M_{F555W} \gtrsim -5.74$ and $M_{F814W} \gtrsim -7.10$.

An age for the environment around SN 2004gt was estimated by comparing the positions of nearby stars on a colour-magnitude diagram with theoretical isochrones (we use the stellar evolution tracks and isochrones of the Geneva stellar evolution group²). The isochrones were shifted for the distance, extinction and reddening of NGC 4038. Assuming the standard Galactic extinction-reddening relationship of $A_V \approx 3.1E(B - V)$ and $E(V - I) = 0.62E(B - V)$, the value of the reddening calculated above yielded $A_V = 0.22 \pm 0.03$ and $E(V - I) = 0.04 \pm 0.01$. The colour-magnitude diagram showing the positions of stars within $0.5''$ of SN 2004gt compared with theoretical isochrones is shown as Fig. 2. The mean age of the nearby stars was measured to be $\log(\text{age}/\text{years}) = 6.93 \pm 0.13$, or $8.5 \pm 2.5\text{Myr}$. This

¹<http://nedwww.ipac.caltech.edu/>

²<http://webast.ast.obs-mip.fr/stellar/>

age is consistent with the age of 7 ± 1 Myr estimated by Whitmore et al. (1999) for knot S. The age of the nearby stars corresponds to the lifetime of stars with $M_{ZAMS} \approx 20 - 40 M_{\odot}$.

4. DISCUSSION

Maund & Smartt (2005), Smartt et al. (2002) and Van Dyk et al. (2003) have shown how the pre-explosion photometry may, in the event of the non-detection of the progenitor, be used to place mass limits on the progenitor. The pre-explosion detection thresholds were converted to luminosity thresholds for a range of supergiant spectral types, using the colours, temperatures and bolometric corrections given by Drilling & Landolt (2000). In addition synthetic photometry was conducted on model WR spectra (Gräfener et al. 2002; Maund & Smartt 2005), using the STSDAS packages *synphot*, to calculate the colours and bolometric corrections for these types of stars. These colours and corrections are dependent on two parameters: the effective temperature and the “Transformed Radius.” Maund & Smartt (2005) discuss how the two-parameter space of model spectra was sampled to completely measure the spread in colours and bolometric corrections. The principal consequence of this two-parameter dependence is that at high temperatures, when the progenitors are expected to be WR stars, the uncertainty in the luminosity increases with temperature compared to the relationship for supergiants. The observed absolute magnitude detection limits were converted to bolometric magnitudes using the expression:

$$\begin{aligned} M_{bol}(T_{eff}) = & M_{X;WFPC2} + (M_{X;J-C} - M_{X;WFPC2}) \\ & + (M_V - M_{X;J-C}) + B.C. \end{aligned} \quad (2)$$

where $X;WFPC2$ and $X;J - C$ indicate magnitudes in a general WFPC2 filter and the corresponding filter in the Johnson-Cousins photometric system, respectively. The luminosities were calculated from the bolometric magnitudes in the standard manner assuming $M_{bol}(\odot) = +4.74$. The detection thresholds for the four different filters were plotted on HR diagrams, shown in Fig. 3, and compared with stellar evolution tracks to estimate mass limits.

The F336W pre-explosion observation does not place a stringent constraint of the progenitor, missing both the red supergiant and blue WR end points of the stellar evolution tracks for low-intermediate and high-mass stars, respectively. The F439W observation excludes yellow and red supergiant progenitors, for $M_{ZAMS} \approx 20 - 25 M_{\odot}$ as well as the lowest mass stars which end their lives with a WR phase ($M_{ZAMS} \approx 25 - 40 M_{\odot}$). The constraint against a WR progenitor, with initial mass of $40 M_{\odot}$, is weak, however, as the luminosity uncertainty is large. The red supergiant progenitors for stars with $M_{ZAMS} < 25 M_{\odot}$ are completely excluded by the F814W observation (including the location of the progenitor of the type IIP

SN 2003gd; Smartt et al. 2004). The F555W observation places much stronger constraints on both sides of the HR diagram. A much tighter constraint on the WR branch excludes a $M_{ZAMS} \approx 25 - 40M_{\odot}$ progenitor. All four pre-explosion observations clearly indicate that the SN 2004gt was not the explosion of a super-massive $M_{ZAMS} \approx 120M_{\odot}$ star. The depth of the observation, despite not being sufficient to detect the progenitor, provides useful limits on the progenitor of SN 2004gt.

The pre-explosion observations do not exclude possible blue lower mass progenitors in binaries, with $M_{ZAMS} = 20 - 40M_{\odot}$ as given by the age determined for the surrounding stellar population. The evolution of such a progenitor would have been affected by angular-momentum and mass exchange with a companion, which would strip the progenitor's H envelope leaving a low-luminosity high-temperature He and C-O star as the progenitor (Podsiadlowski et al. 2004). Maund & Smartt (2005) have suggested this as a possible explanation for the lack of the detection of a number of progenitors of type Ib/c SNe. This progenitor scenario was also invoked by Nomoto et al. (1994) for the type Ic SN 1994I. Podsiadlowski et al. (2004) argue that prompt collapse of a single star would produce a faint SN, whereas SN 2004gt is of normal brightness. The distance to NGC 4038, 19.2Mpc, is prohibitive to conducting a spectroscopic search for the companion (Maund et al. 2004).

In Table 2 we compile all the directly measured upper limits for the magnitudes of the progenitors of SNe Ibc, in various pass-bands. We can determine the upper final mass limit, i.e. the mass *prior* to explosion, of a WR star progenitor from the mass-luminosity relationship of the Langer models (Langer 1989). These upper limits are somewhat higher, although not inconsistent with the calculated final mass of the star which produced SN 2002ap ($5 - 7M_{\odot}$; which includes $\sim 2M_{\odot}$ allowance for a compact remnant) determined from modelling the spectral evolution of the supernova (Mazzali et al. 2002). Vacca & Torres-Dodgen (1990) give the range of observed absolute magnitudes for Galactic WN stars as $M_V = -3.2$ to -8.0 . Assuming a uniform distribution in absolute brightness implies that the pre-explosion observations are sensitive to $\approx 50\%$ of WN stars, mostly WNL stars (Smartt et al. 2002). The luminosities of WC stars in the LMC (Crowther et al. 2002) are $\log(L/L_{\odot}) < 5.8$, which places them within the lower uncertainty boundary for the detection of WR stars (see Fig. 3).

Understanding the progenitors of Type Ic SNe, whether high-mass WR stars or low-mass stars in binaries, is important for understanding the relationship between SNe and GRBs (Hjorth et al. 2003). The high rate of SNe events in the merging galaxies NGC 4038/4039 ($0.2 - 0.3$ SNe yr^{-1} ; Neff & Ulvestad 2000) in conjunction with the large amount of deep imaging of this system available suggests that NGC 4038/4039 is a good candidate for the detection of progenitors of Type Ibc SNe in the future.

5. CONCLUSIONS

The location of SN 2004gt, in the galaxy NGC 4038, in pre-explosion HST WFPC2 images has been identified using differential astrometry with a post-explosion high-resolution HST ACS observation of SN 2004gt. The progenitor location was identified with an accuracy of 5mas. The progenitor was not detected in any of the deep F336W, F439W, F555W and F814W pre-explosion imaging. The detection thresholds of the pre-explosion observations suggest that SN 2004gt arose from a single star progenitor with $M_{ZAMS} \gtrsim 40M_{\odot}$ or a $M_{ZAMS} \approx 20 - 40M_{\odot}$ star in a binary. This is the most restrictive mass limit placed on any type Ib/c SN yet, and this is attributable to the depth of the available pre-explosion imaging.

Based on observations made with the NASA/ESA Hubble Space Telescope and obtained from the Data Archive at the Space Telescope Science Institute, which is operated by the Association of Universities for Research in Astronomy, Inc., under NASA contract NAS 5-26555. These observations are associated with programs GO-5962 and GO-10187. JRM and SJS acknowledge financial support from PPARC. FS acknowledges partial support from the NSF through grant AST02-05994. We thank W. Januszewski for his immense help with coordinating the post-explosion HST ACS observation of SN 2004gt and W.-R. Hamann for providing access to the Potsdam Wolf-Rayet Models.

REFERENCES

Aldering, G., Humphreys, R. M., & Richmond, M. 1994, AJ, 107, 662

Crowther, P. A., Dessart, L., Hillier, D. J., Abbott, J. B., & Fullerton, A. W. 2002, A&A, 392, 653

Dolphin, A. E. 2000a, PASP, 112, 1397

—. 2000b, PASP, 112, 1383

Drilling, J. S., & Landolt, A. U. 2000, in Allen's Astrophysical Quantities, 4th edn., ed. A. N. Cox (New York: AIP)

Eldridge, J. J., & Tout, C. A. 2004, MNRAS, 353, 87

Ganeshalingam, M., Swift, B. J., & Filippenko, A. V. 2004, IAUC, 8456, 3

Gräfener, G., Koesterke, L., & Hamann, W.-R. 2002, A&A, 387, 244

Heger, A., Fryer, C. L., Woosley, S. E., Langer, N., & Hartmann, D. H. 2003, *ApJ*, 591, 288

Hjorth, J., & et al. 2003, *Nature*, 423, 847

Holtzman, J. A., Burrows, C. J., Casertano, S., Hester, J. J., Trauger, J. T., Watson, A. M., & Worthey, G. 1995, *PASP*, 107, 1065

Krist, J., & Hook, R. 2004, The Tiny Tim User's Guide, 6th edn., <http://www.stsci.edu/software/tinytim>

Langer, N. 1989, *A&A*, 220, 135

Matheson, T., & et al., D. 2003, *ApJ*, 599, 394

Maund, J. R., & Smartt, S. J. 2005, *MNRAS*, 360, 288

Maund, J. R., Smartt, S. J., Kudritzki, R. P., Podsiadlowski, P., & Gilmore, G. F. 2004, *Nature*, 427, 129

Mazzali, P. A., & et al. 2002, *ApJL*, 572, L61

Monard, L. A. G., Quimby, R., Gerardy, C., Hoeflich, P., Wheeler, J. C., Chen, Y.-T., Smith, H. J., & Bauer, A. 2004, *IAUC*, 8454, 1

Neff, S. G., & Ulvestad, J. S. 2000, *AJ*, 120, 670

Nomoto, K., Yamaoka, H., Pols, O. R., van den Heuvel, E. P. J., Iwamoto, K., Kumagai, S., & Shigeyama, T. 1994, *Nature*, 371, 227

Podsiadlowski, P., Mazzali, P. A., Nomoto, K., Lazzati, D., & Cappellaro, E. 2004, *ApJL*, 607, L17

Riess, A., & Mack, J. 2004, Time Dependence of ACS WFC CTE Corrections for Photometry and Future Predictions, *Instrument Science Report ACS 2004-006*, Space Telescope Science Institute

Schlegel, D. J., Finkbeiner, D. P., & Davis, M. 1998, *ApJ*, 500, 525

Sirianni, M., Jee, M. J., Benítez, N., Blakeslee, J. P., Martel, A. R., Clampin, M., de Marchi, G., C., F. H., & et al., 2005, *PASP*

Smartt, S. J., Maund, J. R., Hendry, M. A., Tout, C. A., Gilmore, G. F., Mattila, S., & Benn, C. R. 2004, *Science*, 303, 499

Smartt, S. J., Vreeswijk, P. M., Ramirez-Ruiz, E., Gilmore, G. F., Meikle, W. P. S., Ferguson, A. M. N., & Knapen, J. H. 2002, ApJL, 572, L147

Vacca, W. D., & Torres-Dodgen, A. V. 1990, ApJS, 73, 685

Van Dyk, S. D., Li, W., & Filippenko, A. V. 2003, PASP, 115, 1

Van Dyk, S. D., Peng, C. Y., Barth, A. J., & Filippenko, A. V. 1999, AJ, 118, 2331

Walborn, N. R., Prevot, M. L., Prevot, L., Wamsteker, W., Gonzalez, R., Gilmozzi, R., & Fitzpatrick, E. L. 1989, A&A, 219, 229

Whitmore, B. C., Zhang, Q., Leitherer, C., Fall, S. M., Schweizer, F., & Miller, B. W. 1999, AJ, 118, 1551

This preprint was prepared with the AAS L^AT_EX macros v5.2.

Fig. 1.— Pre- and Post-explosion images of the site of SN 2004gt in NGC 4038. The same orientation is used for all three panels, with North along the y axis and East to the left. SN 2004gt is located at the centre of each of the panels. a) Post-explosion ACS/HRC F555W image, with SN 2004gt clearly visible at (0,0). b) Post-explosion ACS/HRC F814W image. c) Pre-explosion WFPC2 PC chip F555W image, transformed, shifted and rotated to the coordinates of the post-explosion ACS imaging. No object is significantly detected at the position of SN 2004gt prior to explosion, with a positional uncertainty 0.004''. The plate scale of the pre- and post-explosion images is 0.025''. In these images knot S appears in the top-right. A small “light echo” is apparent around the SN in the post-explosion images, from reflections of the SN off dust in NGC 4038.

Table 1: Pre- and post-explosion HST observations of SN 2004gt site in NGC 4038.

Date	JD (2450000+)	Filter	Instrument	Exposure Time(s)	HST Programme
1996 Jan 20	102.45	F336W	WFPC2 (PC)	4500	GO-5962
1996 Jan 20	102.51	F439W	WFPC2 (PC)	4000	GO-5962
1996 Jan 20	102.58	F555W	WFPC2 (PC)	4400	GO-5962
1996 Jan 20	102.65	F814W	WFPC2 (PC)	2000	GO-5962
2005 May 16	3506.25	F435W	ACS (HRC)	1672	GO-10187
2005 May 16	3506.18	F555W	ACS (HRC)	1530	GO-10187
2005 May 16	3506.20	F814W	ACS (HRC)	1860	GO-10187

Table 2: Compilation of all the directly determined limits to the progenitors of SNe Ibc.

Supernova	Type	Limiting magnitudes					$\log L$ (L_\odot)	M_{Final} (M_\odot)
		M_U	M_B	M_V	M_R	M_I		
2000ds	Ib	-6.0	...	-6.5	5.2	10
2000ew	Ic	-6.4	5.5	15
2001B	Ib	-8.0	6.0	25
2002ap	Ic	-8.7	-6.8	-7.2	-7.8	-8.4	5.6	18
2004gt	Ic	-8.42	-6.82	-5.31	...	-6.77	5.1	9

NOTES.— Limits are from this paper, Smartt et al. (2002), and Maund & Smartt (2005). The limiting magnitudes for SN 2002ap have been adjusted for the new large distance to M74 as determined by Hendry et al. (2005). The M_V and M_I magnitudes for SN 2000ds are HST M_{F555W} and M_{F814W} ; M_V for SN 2000ew and SN 2001B are M_{F606W} and M_{F555W} respectively. For SN 2004gt the limiting magnitudes M_U , M_B , M_V and M_I are HST M_{F336W} , M_{F439W} , M_{F555W} and M_{F814W} respectively.

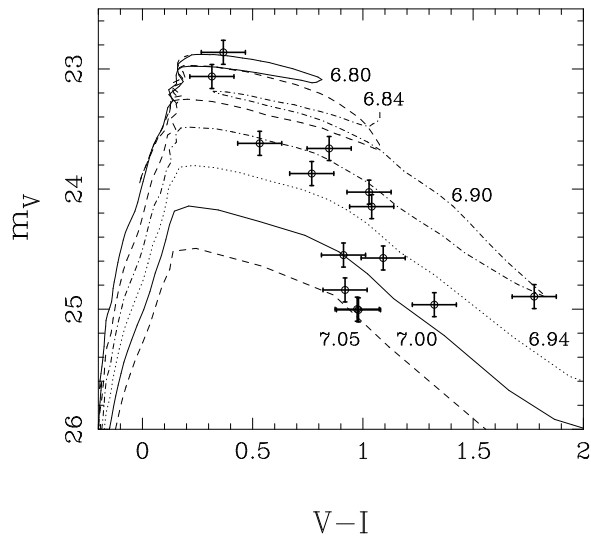


Fig. 2.— Colour-magnitude diagram showing stars within $0.5''$ of SN 2004gt in NGC 4038. Overlaid are solar metallicity Geneva isochrones (with extended mass loss rates), shifted for the distance, extinction and reddening to SN 2004gt. The locations of the stars on this figure correspond to an age of $\log(\text{age}/\text{years}) = 6.93 \pm 0.13$.

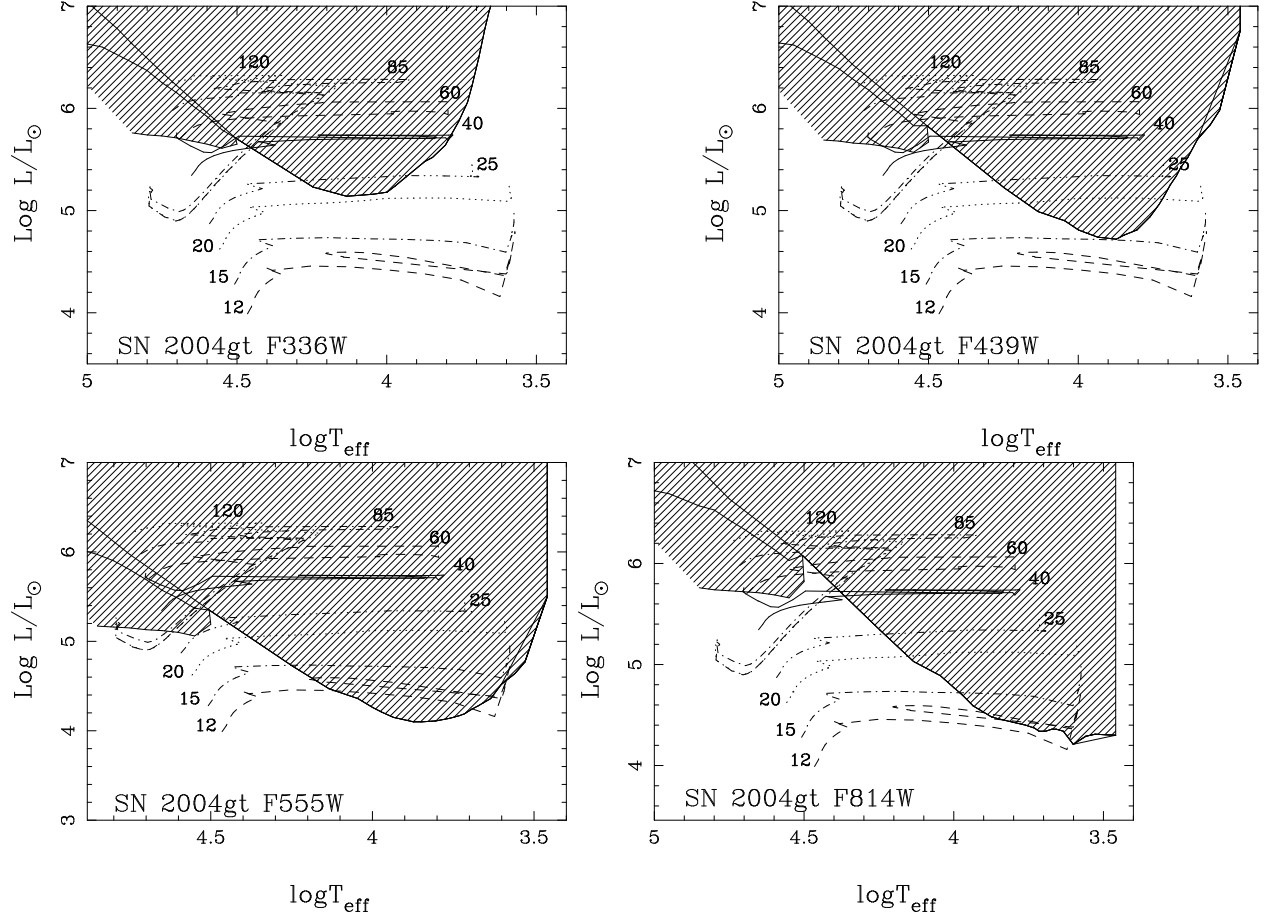


Fig. 3.— Hertzsprung-Russell diagrams showing solar metallicity stellar evolution tracks. Overlaid are the detection thresholds for the pre-explosion HST WFPC2 F336W, F439W, F555W and F814W images. A progenitor lying in the grey regions would have been significantly detected on the pre-explosion images.

This figure "fig1a.jpg" is available in "jpg" format from:

<http://arxiv.org/ps/astro-ph/0506436v1>

This figure "fig1b.jpg" is available in "jpg" format from:

<http://arxiv.org/ps/astro-ph/0506436v1>

This figure "fig1c.jpg" is available in "jpg" format from:

<http://arxiv.org/ps/astro-ph/0506436v1>